OPEN

Citation: Blood Cancer Journal (2017) **7**, e572; doi:10.1038/bcj.2017.51

www.nature.com/bcj

ORIGINAL ARTICLE

The thrombopoietin/MPL axis is activated in the *Gata1^{low}* mouse model of myelofibrosis and is associated with a defective RPS14 signature

M Zingariello[1], L Sancillo[2], F Martelli[3], F Ciaffoni[3], M Marra[3], L Varricchio[4], RA Rana[2], C Zhao[5], JD Crispino[5] and AR Migliaccio[4,6]

Myelofibrosis (MF) is characterized by hyperactivation of thrombopoietin (TPO) signaling, which induces a RPS14 deficiency that de-regulates GATA1 in megakaryocytes by hampering its mRNA translation. As mice carrying the hypomorphic *Gata1^{low}* mutation, which reduces the levels of *Gata1* mRNA in megakaryocytes, develop MF, we investigated whether the TPO axis is hyperactive in this model. *Gata1^{low}* mice contained two times more *Tpo* mRNA in liver and TPO in plasma than wild-type littermates. Furthermore, *Gata1^{low}* LSKs expressed levels of *Mpl* mRNA (five times greater than normal) and protein (two times lower than normal) similar to those expressed by LSKs from TPO-treated wild-type mice. *Gata1^{low}* marrow and spleen contained more JAK2/STAT5 than wild-type tissues, an indication that these organs were reach of TPO-responsive cells. Moreover, treatment of *Gata1^{low}* mice with the JAK inhibitor ruxolitinib reduced their splenomegaly. Also in *Gata1^{low}* mice activation of the TPO/MPL axis was associated with a RSP14 deficiency and a discordant microarray ribosome signature (reduced *RPS24*, *RPS26* and *SBDS* expression). Finally, electron microscopy revealed that *Gata1^{low}* megakaryocytes contained poorly developed endoplasmic reticulum with rare polysomes. In summary, *Gata1^{low}* mice are a bona fide model of MF, which recapitulates the hyperactivation of the TPO/MPL/JAK2 axis observed in megakaryocytes from myelofibrotic patients.

Blood Cancer Journal (2017) **7,** e572; doi:10.1038/bcj.2017.51; published online 16 June 2017

INTRODUCTION

A number of studies have shown that the myeloproliferative neoplasm myelofibrosis (MF) is caused by genetic abnormalities involving the thrombopoietin (TPO) axis, including mutations in *JAK2*, the TPO receptor *MPL* or in calreticulin (*CALR*).[1] All three classes of mutations lead to hyperactive JAK/STAT signaling. Furthermore, patients with MF also have elevated serum TPO levels.[2] These mutations, however, are also found in the related myeloproliferative neoplasm diseases polycythemia vera and essential thrombocythemia, prompting the hypothesis that the disease phenotype is determined by a genetic modifier yet to be identified. The observation that MF is specifically associated with reduced GATA1 content in megakaryocytes[3] has suggested that this abnormality may be a phenotypic modifier in MF. The 'element' that specifically links TPO signaling with de-regulated GATA1 expression in megakaryocytes is, therefore, subject of investigation. We have recently presented data suggesting that this 'element' is represented by enrichment of ribosomal pathways gene signatures, which was associated with impaired GATA1 translation in megakaryocytes[4,5]

Support for the role of GATA1 deficiency in megakaryocytes as the 'phenotype modifier' in MF was provided by the observation that mice carrying a hypomorphic mutation (*Gata1^{low}*) that deletes the hypersensitive site (HS1), which drives transcription of *Gata1* in megakaryocytes,[6] develop MF.[7] Although *Gata1^{low}* mice are not anemic,[7] they are subjected to continuous erythroid stress due to the reduced half-life of their erythrocytes.[8] The animals recover from this stress by activating an alternative erythroid differentiation pathway in the spleen, which involves the production of specific bipotent erythroid/megakaryocyte precursors.[8,9] The phenotype of the stress precursors identified in *Gata1^{low}* mice is different from that identified by Paulson *et al.*,[10] which is induced by acute stress, and is similar to that of the bipotent erythroid/megakaryocyte precursors generated *in vitro* by human CD34+ cells in response to a chemical MPL hyperstimulator,[11] leading us to investigate the activation status of the TPO/MPL axis in this model.

MATERIALS AND METHODS

Mice

Male wild-type and *Gata1^{low}* mice were originally obtained from Dr S Orkin[12] and outbread in the animal facility of Istituto Superiore di Sanità as described.[7,13] Littermates were genotyped at birth by PCR,[13] and those found not to carry the mutation were used as wild-type controls. *Mpl^{null}* mice were provided by Dr W Alexander.[14] All the experiments were performed according to the protocols approved by the institutional animal care committee according to the European Directive 86/609/EEC.

Treatments

Bleeding. A volume of 200 μl of blood was collected from wild-type mice through the retro-orbital plexus. Mice were killed by cervical dislocation 24 h later and their tissues removed for further analyses.

[1]Department of Medicine, Campus Biomedico, Rome, Italy; [2]Medicine and Aging Science, University of Chieti G. D'Annunzio, Chieti, Italy; [3]Hematology/Oncology and Molecular Medicine, Istituto Superiore di Sanità, Roma, Italy; [4]Tisch Cancer Institute, Icahn School of Medicine at Mount Sinai (ISMMS), New York, NY, USA; [5]Division of Hematology/Oncology, Northwestern University, Chicago, IL, USA and [6]Department of Biomedical and Neuromotorial Sciences, Alma Mater University, Bologna, Italy. Correspondence: Dr AR Migliaccio, Department of Medicine, Icahn School of Medicine at Mount Sinai (ISMMS), One Gustave L Levy Place, Box #1079, New York, NY 10029, USA.
E-mail: annarita.migliaccio@mssm.edu
Received 18 April 2017; accepted 2 May 2017

TPO treatment. Wild-type mice (9–10 months old) were treated intraperitoneally with of TPO (100 μg/kg/day for 5 days in saline).

Ruxolitinib. Nine- to ten-month-old *Gata1^{low}* mice (four males and four females per experimental group) were treated with Ruxolitinib (Rux; #S1378 INCB 018424; Selleckchem, Houston, TX, USA; 45 mg/kg twice per day by gavage in 2% v/v dimethylsulfoxide in H_2O) and vehicle (2% v/v dimethylsulfoxide in H_2O) for 5 consecutive days, rested for 2 days and then treated for 5 additional days.[15] On day 17, mice were weighed, bled for blood parameters determinations and killed for organ histopathology observations. Results are compared with those observed in historic wild-type controls.[16,17] Hematocrit and platelet counts were determined manually.

Flow cytometry and cell sorting

Lineage negative cells were labeled with fluorescein isothiocyanate-conjugated Scal, phycoerythrin-conjugated anti-CD117 (cKit) (LSK cells) and anti-MPL antibody (AMM2, Kirin Pharmaceuticals, Tokyo, Japan)[18,19] or irrelevant isotype-matched antibodies. Cell fluorescence was analyzed with a FACS ARIA cell sorter (Becton Dickinson, Franklin Lakes, NJ, USA) and expressed as mean fluorescent intensity. LSK were isolated as described.[20]

Enzyme-linked immunosorbent assay for TPO

The levels of TPO present in platelet-poor plasma and organ washes were measured by enzyme-linked immunosorbent assay (Quantikine Immunoassay mouse TPO; R&D Systems, Inc., Minneapolis, MN, USA), according to the manufacturer's instructions. Platelet-poor plasma was prepared by centrifugation at 5000 r.p.m.; blood collected with ethylenediaminetetraacetic acid-coated microcapillary tubes (20–40 μl/sampling). Organ washes were prepared as described.[21]

RNA isolation, quantitative reverse transcription-PCR and microarray analyses

Total RNA was prepared with Trizol (Gibco-BRL, Grand Island, NY, USA) and reverse transcribed with random primers using the superscript III kit (Invitrogen Life Technologies, Bethesda, MD, USA). Gene expression levels were quantified by quantitative reverse transcription-PCR using TaqMan Universal PCR Master Mix (Applied Biosystems, Carlsbad, CA, USA) and commercial primers (inventoried TaqMan Gene Expression Assays (Applied Biosystems). GAPDH or β-actin were used as control as described by the manufacturer. Reactions were performed in an ABI 7300 Real Time PCR System (Applied Biosystems). Cycle threshold (Ct) was calculated with the SDS software Version 1.3.1 (Applied Biosystems), and mRNA levels were expressed as $2^{-\Delta Ct}$ (ΔCt = target gene Ct − GAPDH Ct). For microarray analyses, total RNA was extracted from the bone marrow and spleen of 8- to 10-month-old *Gata1^{low}* and wild-type littermates and purified with Rneasy Mini Kit (Qiagen, Germantown, MD, USA). Hybridization to Illumina Mouse WG-6V2 Bead Chip gene expression array was performed by the Microarray Resource Facility, Icahn School of Medicine at Mount Sinai. Functional Annotation Clustering was performed with the David Bioinformatic Database (David Bioinformatics Resources 6.7 NIAID/NIH). Microarray data have been deposited in the Gene Expression Omnibus database (GSE89630) https://www.ncbi.nlm.nih.gov/geo/query/acc.cgi?token=ijgpwgsyjhwpdoj&acc=GSE89630.

Western blot analysis

Protein extracts separated on SDS-polyacrylamide gel electrophoresis, were blotted on nitrocellulose membranes and probed with antibodies against JAK2 (D2E12 #3230), pSTAT5 (#9351), Ezh2 (Ac22 #3147), SMAD2/3 (#5339), p38 (#9213) and p-p38 (T180/Y182 #4511) (all from Cell Signaling, Boston, MA, USA), STAT5 (#sc-835, Santa Cruz Biotechnology, Santa Cruz, CA, USA) and GAPDH (#CB1001, Calbiochem, San Diego, CA, USA).

Histology

Tissues were fixed in 10% (v/v) phosphate-buffered formalin according to standard procedures,[16] paraffin-embedded and cut into consecutive 2.5–3 μm sections that were then stained either with either hematoxylin–eosin and Gomori silver (MicroStain MicroKit, Bologna, Italy), or immunostained with anti-transforming growth factor (TGF)-β1 (sc-146, Santa Cruz Biotechnology) antibodies. Immunoreactions were detected with STAT-Q Peroxidase–AEC Staining System Kit (Innovex Biosciences, Richmond, CA, USA). Images acquired with the Light microscope (ZEISS, Axioskop, Germany) equipped with a Coolsnap Videocamera were quantified with the MetaMorph 6.1 Software (Universal Imaging Corp., Downingtown, PA, USA). Electron microscopyand immuno-electron microscopy observations were performed as described previously.[16,17]

Statistical analyses

Results were analyzed by analysis of variance (Windows Origin 6.0, Microcal Software Inc., North Hampton, MA, USA), Wilcoxon–Mann–Whitney test (two-sided) or multi-regression modeling (SAS software v9.2, SAS Institute, Cary, NC, USA). For microarray, Bonferroni-corrected *P*-values < 0.05 were regarded as a statistically significant association. Gene set enrichment analysis was used to identify pathways that were altered in *Gata1^{low}* mice as described.[22]

RESULTS

Gata1^{low} mice express high levels of TPO

TPO mRNA was expressed not only, as expected,[23] by the liver and kidney but also by all hematopoietic tissues (spleen, bone marrow and bone) and tissues containing TPO-responsive mast cells (ear, stomach and intestine)[24,25] both *Gata1^{low}* mice and wild-type littermates (Table 1). In wild-type mice, the greatest levels of TPO mRNA were detected in the liver (>30-fold than any other tissue), followed by kidney and intestine. The liver and stomach from *Gata1^{low}* mice expressed levels of TPO mRNA 2- to 3-fold greater than normal while TPO mRNA levels were 10-fold lower than normal in their bone, bone marrow and spleen. This altered pattern of TPO mRNA tissue distribution appears to be unique to *Gata1^{low}* mice as bleeding or genetic *Mpl* ablation had modest effects on the levels of TPO mRNA expressed by tissues from mice wild type at the *Gata1* locus. The great levels of TPO mRNA expressed by the liver from *Gata1^{low}* mice are consistent with the great levels of interleukin-6, the major regulator of TPO production by the liver,[26] expressed by these mutants.[16]

By enzyme-linked immunosorbent assay, TPO protein was detected in the plasma and in washes from all the tissues investigated (bone marrow, spleen, liver and peritoneum; Table 1). As expected[27,28] the greatest levels of TPO protein were detected in the plasma, and these levels were increased by bleeding (by 30%) and *Mpl* (by threefold) ablation.[29] Also the plasma from *Gata1^{low}* mice contained levels of TPO threefold higher than normal (778 ± 101 vs 351 ± 31 pg/ml) and only two times lower than those of the plasma from mice carrying the *Mpl^{null}* mutation (1287 ± 205 pg/ml; Table 1).

The plasma concentration of TPO is mainly regulated by intracellular degradation following binding to its receptor Mpl by megakaryocytes[30] and platelets.[31] The increased production of TPO mRNA by the liver and the greater than normal TPO concentration in the plasma of *Gata1^{low}* mice in spite of the numerous megakaryocytes expressing surface levels of MPL two times greater than normal (MPL mean fluorescence intensity ~ 200 vs 600 per wild-type and *Gata1^{low}* CD61+CD41+ cells, respectively) present in their bone marrow and spleen indicate that *Gata1^{low}* mice contain levels of TPO greatly higher than normal and possibly similar to those reported to induce fatal MF in mice (range 800–8000 pg/ml).[32]

In conclusion, *Gata1^{low}* mice express high levels of TPO mRNA in the liver and levels of TPO protein in plasma similar to those which induce MF in mice.

LSK from *Gata1^{low}* mice express a MPL pattern suggestive of receptor activation

We next compared the levels of MPL (mRNA and protein) expressed by LSK from *Gata1^{low}* and wild-type littermates (Figures 1a–c). Although *Gata1^{low}* LSK contained levels of Mpl mRNA three times greater than that expressed by wild-type cells,

Table 1. The liver and the plasma from *Gata1^{low}* mice express greater levels of TPO mRNA and protein than that of piastrinopenic mouse models (bled wild-type mice and *Mpl^{null}* mice)

	Wild type	*Wild type, bleeding*	*Gata1^{low}*	*Mpl^{null}*
Blood values				
Hct (%)	47.8 (±0.3)	43.1 (±1.1)[a]	45.0 (±3.3)	42.3 (±1.3)[a]
Plt/μl (×10^6)	0.9 (±0.03)	0.7 (±0.03)[a]	0.3 (±0.01)[†]	0.03 (±0.004)[a]
TPO mRNA ($2^{-\Delta Ct}$)(×10^{-3})				
Liver	39.3 ± 7	41.3 ± 4.3	94.2 ± 9.5[a]	35.5 ± 10.5
Spleen	1.3 ± 0.1	0.5 ± 0.2	0.02 ± 0.002[a]	ND
Bone marrow	0.1 ± 0.006	3 ± 1[a]	0.007 ± 0.001[a]	0.01 ± 0.002[a]
Bone	1.9 ± 0.5	0.5	0.3 ± 0.1[a]	BD
Ear	BD	1.2	0.06 ± 0.005	BD
Kidney	6.2 ± 0.001	7.6 ± 0.9	10.6 ± 1.3	8.9 ± 2.1
Stomach	0.7 ± 0.1	0.3 ± 0.03[a]	4.6 ± 0.9[a]	1.0 ± 0.1
Intestine	4.0 ± 0.2	8.2 ± 2.0	2.9 ± 0.7	2.2 ± 0.1[a]
TPO protein (pg/ml)				
Plasma	351 ± 31[a]	451 ± 11[a]	778 ± 101[a]	1287 ± 205
Bone marrow	98 ± 13	96 ± 14[a]	25 ± 1[a]	47 ± 13
Spleen	99 ± 15	140 ± 4	66 ± 3	119 ± 7
Liver	289 ± 28	179 ± 6[a]	166 ± 10[a]	271 ± 74
Peritoneum	93 ± 2	88 ± 3	45 ± 5[a]	97 ± 15

Abbreviations: BD, below detection; Hct, hematocrit; ND, not done; Ptl, platelet counts; TPO, thrombopoietin. Blood values and TPO mRNA and protein levels in tissues from wild-type and *Gata1^{low}* and *Mpl^{null}* piastrinopenic mice. Results are presented as mean (±s.d.) of those obtained with three mice per experimental group. [a]Value statistically different ($P < 0.01$ by analysis of variance) from those observed in wild-type mice.

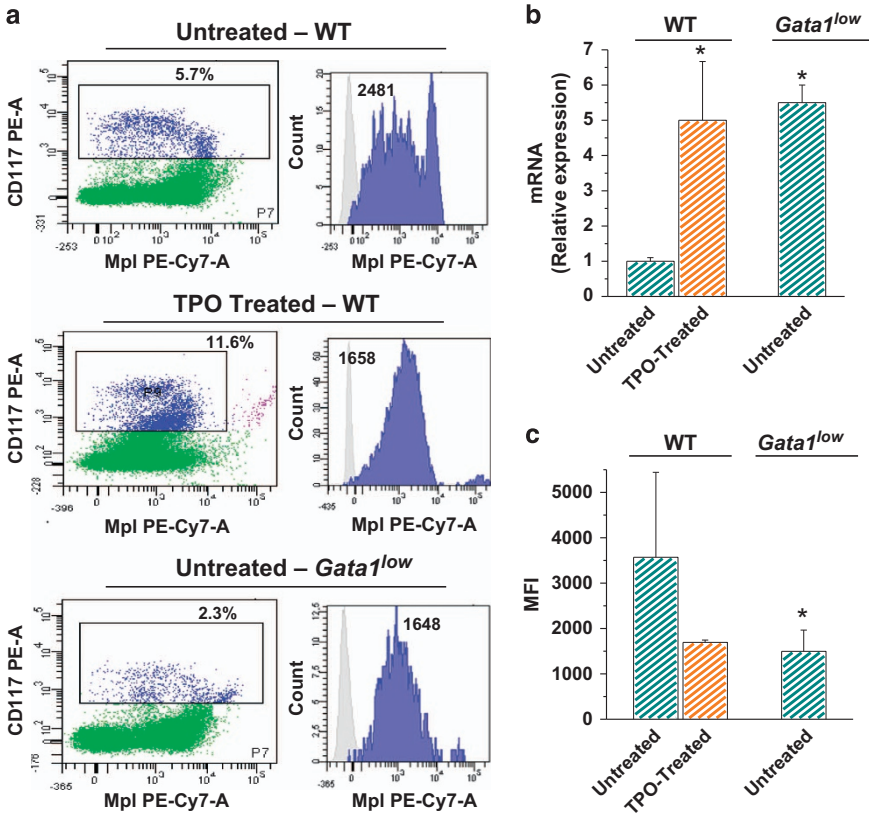

Figure 1. The TPO/MPL axis is activated in LSK from *Gata1^{low}* mice. (**a**) Representative flow cytometry determinations of cell-surface expression of Mpl in Lin^{neg}Sca1$^+$Kit$^+$ (LSK) cells from wild-type mice, either untreated or treated with TPO, and untreated *Gata1^{low}* mice. (**b**) Quantitative reverse transcription-PCR determinations of the levels of *Mpl* mRNA expressed by LSK cells from wild-type mice, either untreated or treated with TPO, and from untreated *Gata1^{low}* mice (six mice per experimental group). Results are expressed as mean (±s.d.) of relative values when compared to those from untreated wild-type mice. (**c**) Mean fluorescence intensity (MFI) determinations of the cell-surface expression of MPL by LSK cells in the same groups analyzed in **a**. Results are expressed as mean (±s.d.) with six mice per experimental point. *$P < 0.05$ with respect to wild-type mice by analysis of variance.

their MPL surface expression was two times lower than that of LSK cells from untreated wild-type mice. Similar increments in levels of *Mpl* mRNA and decrements in levels of MPL cell-surface expression were observed with LSK from wild-type mice subjected to TPO treatment. As with other hematopoietic growth factors, TPO engaging to MPL results in receptor downmodulation followed by activation of *de novo* gene translation.[33] Therefore, the similarity in the levels of *Mpl* mRNA and cell-surface protein observed between TPO-treated and *Gata1^{low}* LSK indicates that the MPL signaling in LSK from *Gata1^{low}* mice is hyperactive. Of note, also CD34+ cells from MF patients express cell-surface MPL levels lower than normal[34] possibly resulting from exposure to TPO levels greater than normal[3] and may indicate pathway hyperactivation as well.[35,36]

Bone marrow and spleen from *Gata1^{low}* mice contain levels greater than normal of signaling elements downstream to the TPO and TGF-β signaling

To assess the cellular consequences of TPO/MPL activation in *Gata1^{low}* mice, the content of its downstream partners JAK2 and STAT5 of bone marrow and spleen from *Gata1^{low}* and wild-type littermates was compared by western blot analyses (Figures 2a and b). JAK2, STAT5 and pSTAT5 were barely detectable in the bone marrow from wild-type mice but were strikingly elevated in that from the mutant animals. JAK2, and to a lesser extent pSTAT5 staining was also elevated in the spleen from *Gata1^{low}* mice. These results suggest that the cellular compartments that respond to TPO are elevated in the bone marrow and spleen from *Gata1^{low}* mice.

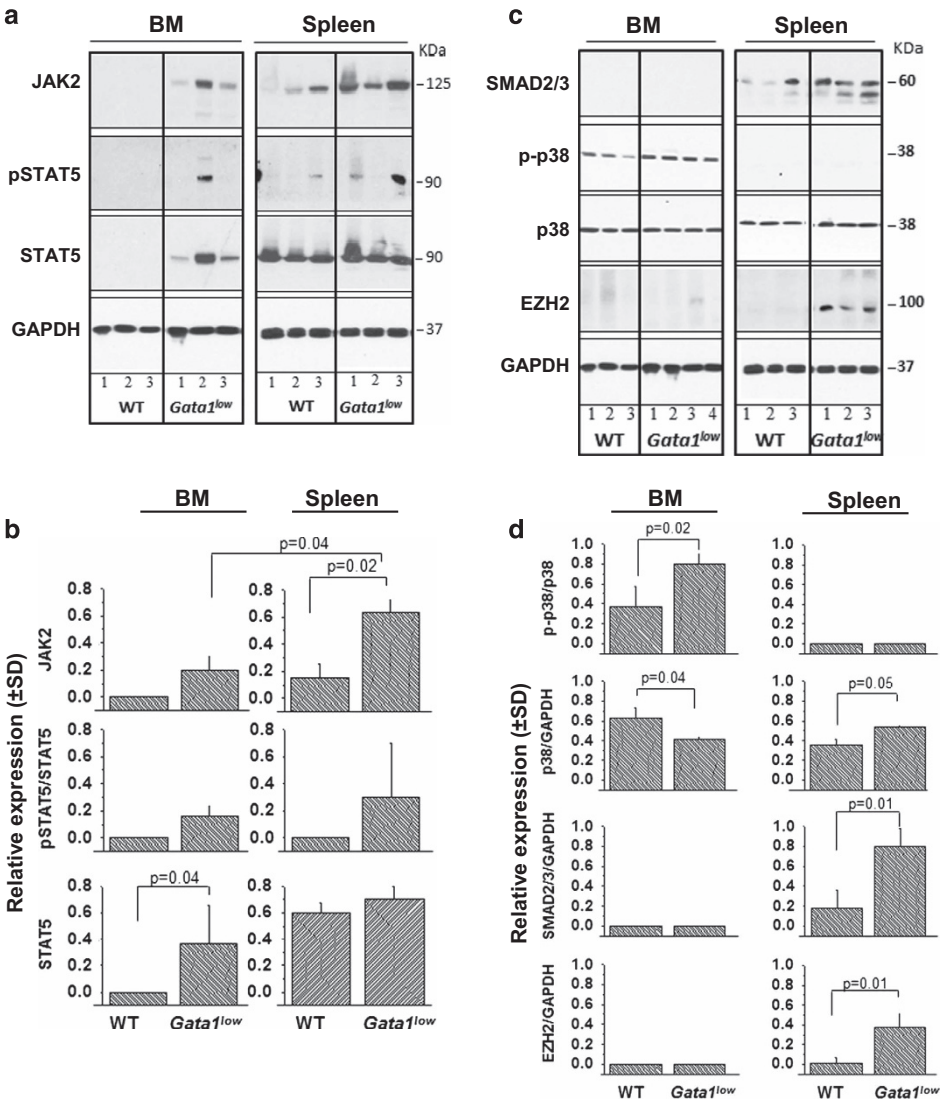

Figure 2. Bone marrow and spleen from *Gata1^{low}* mice contain levels greater than normal both of signaling elements downstream to TPO and of those downstream to TGF-β. (**a**, **b**) Western blot determinations of the JAK2, STAT5 and pSTAT5 content of bone marrow and spleen from wild-type and *Gata1^{low}* mice (each lane). GAPDH was used as loading control. Quantification was obtained by normalizing each band to the corresponding GAPDH level and is presented as mean (±s.d.) with three mice per experimental group. *P*-values were determined by analysis of variance (ANOVA). (**c**, **d**) Western blot determinations of the SMAD2/3, phosphorylated p38 (p-p38), p38 and EZH2 content in the bone marrow and spleen from wild-type and *Gata1^{low}* mice (each line a different mouse). GAPDH was used as a loading control. Quantification was obtained by normalizing p-p38 toward the corresponding p38 band, and SMAD2/3, p38 and EZH2 signals against GAPDH. *P*-values were calculated by ANOVA. EZH2, enhancer of zeste homolog 2.

We have previously shown that *Gata1^{low}* mice, as MF patients, express levels of TGF-β greater than normal and an activated TGF-β signaling profile.[37,38] To compare the cellular alterations induced by TPO and TGF-β activation, the content of elements of the canonical (SMA2/3) and non-canonical (p38) TGF-β signaling, in the bone marrow and spleen from wild-type and *Gata1^{low}* littermates was also evaluated (Figures 2c and d). *Gata1^{low}* mice express levels of p38 phosphorylation two times greater than normal in the bone marrow and of SMAD2/3 two times greater than normal in the spleen. Interestingly, the histone-lysine *N*-methyltransferase enzyme enhancer of zeste homolog 2, which is part of the polycomb repressive complex 2 subunit activated by nuclear factor-kB downstream to the p38 pathway,[39] was also expressed at levels >10 times greater than normal in the spleen suggesting that although undetected by our analyses, the p38 pathway is also activated in the spleen from *Gata1^{low}* mice.

Together these results show that the cellular compartments that respond to TPO are mostly expanded in the bone marrow while those that respond to TGF-β are mostly expanded in the spleen from *Gata1^{low}* mice.

Rux reduces extramedullary hematopoiesis but does not halt disease progression in *Gata1^{low}* mice

The role exerted by JAK2 on the myelofibrotic phenotype expressed by *Gata1^{low}* mice was assessed by treating three females and three males with the Food and Drug Administration-approved JAK inhibitor Rux. Rux also had little effect on the body weight but gave rise to reduced hematocrit and modestly increased platelet counts in the female group (Figures 3a and b).

The treatment had little effect on the JAK2/STAT5 protein content within the bone marrow (data not shown) and on the STAT5 content of the spleen, but led to a twofold reduction in JAK2 within the spleen (Figure 3c), suggesting that the treatment had little effects of the cellular composition of the bone marrow but reduced the cells in the spleen, which express JAK2. In agreement with this interpretation, Rux led to a remarkable reduction in spleen size (with respect to both weight and cell number) and restored the splenic architecture both in females and males (Table 2 and Figure 3d). However, it had no effect on bone marrow cellularity, which remained lower than normal (Table 2). Rux also had no effect on the frequency of megakaryocytes in the bone marrow, which remained greater than normal, but decreased the frequency of these cells in the spleen (Figures 3d and e). Finally, Rux modestly reduced fibrosis in the bone marrow but not in the spleen (Figures 3d and e). The modest effects exerted by Rux on fibrosis were confirmed by the presence of similar great number of tear drop poikilocytes, that is, reticulocytes with the typical morphological deformation acquired when they pass through fibrotic meshes, observed in blood from vehicle- and Rux-treated mice (data not shown).

We had previously confirmed that in *Gata1^{low}* mice altered levels of TGF-β are causative for MF by demonstrating that treatment with an inhibitor of the TGF-β receptor 1 kinase AKL5

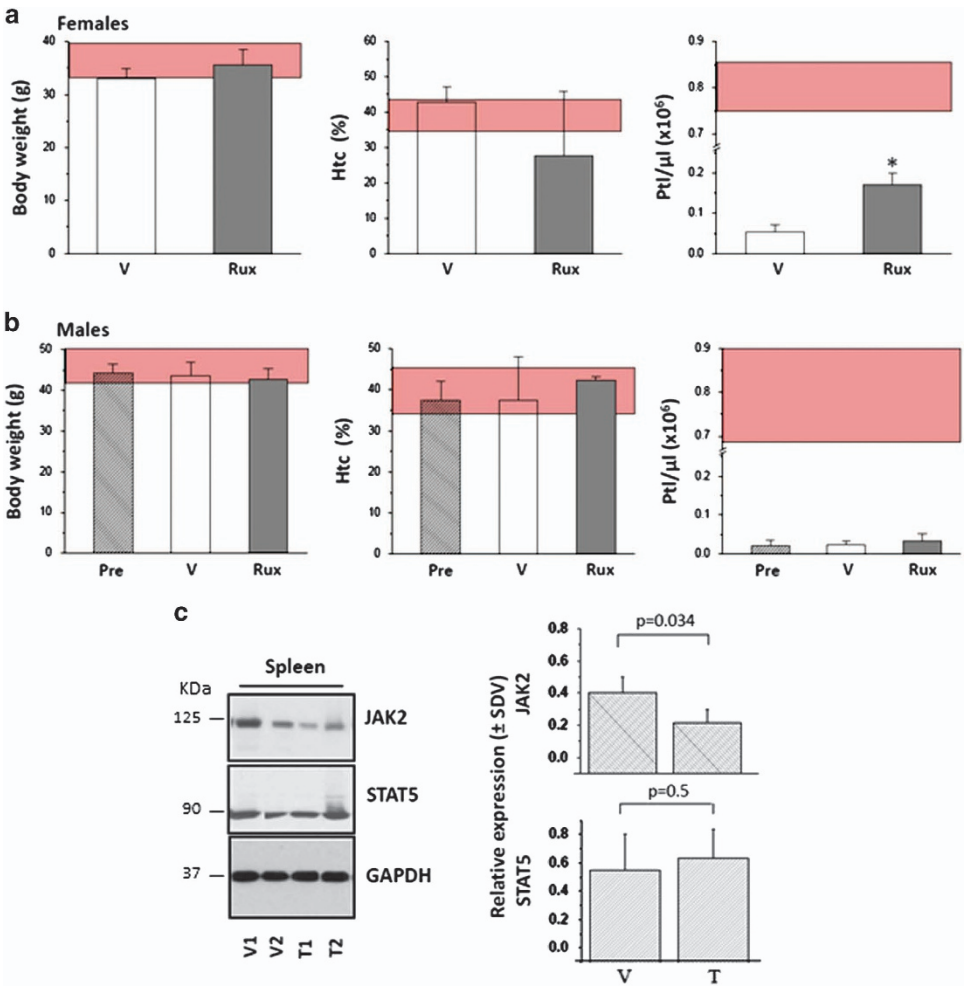

Figure 3. See next page for caption.

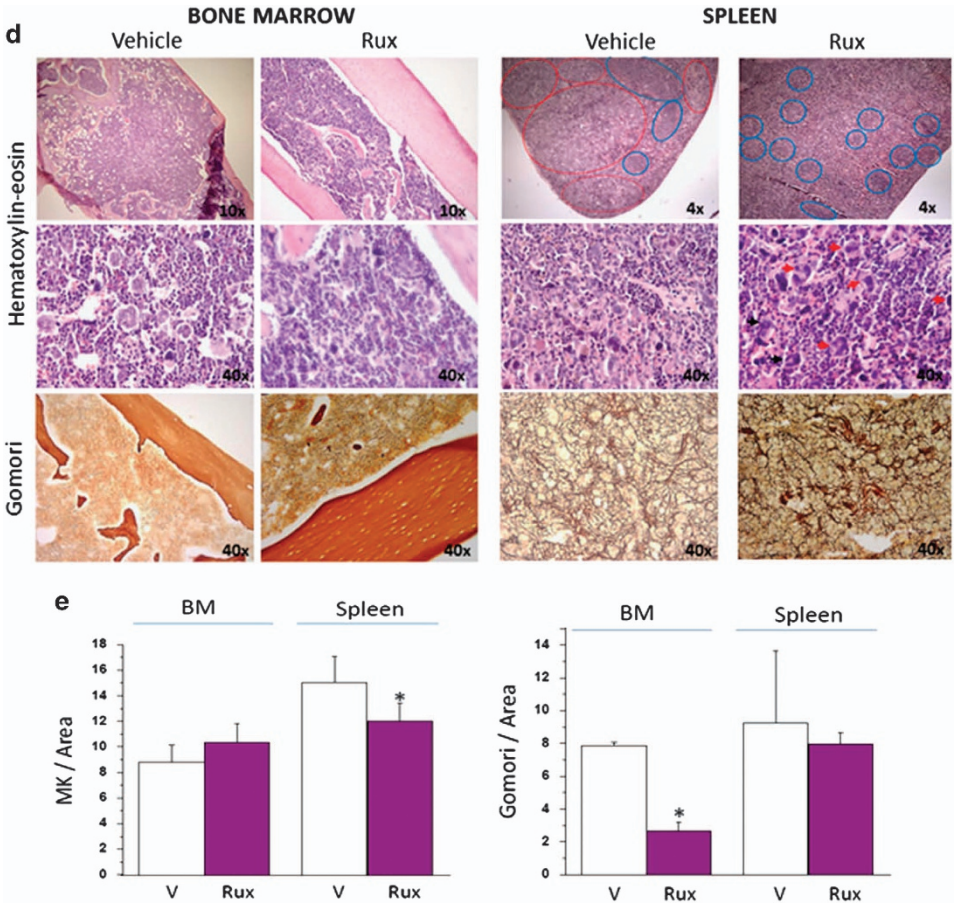

Figure 3. Treatment with Rux reduces JAK2 and restores the architecture of the spleen of *Gata1^{low}* mice. (**a**, **b**) Determination of body weight, hematocrit (Htc) and platelet counts (Ptl) in female (**a**) and male (**b**) *Gata1^{low}* mice treated for 2 weeks with either vehicle (V) or Rux, as indicated. For the group of males, determinations observed before treatment (pre) are also depicted. Results are presented as mean (±s.d.) with three mice per group and are compared with mean (±s.d.) observed in historic wild-type littermates, indicated by the horizontal boxes. *$P < 0.05$ (by analysis of variance (ANOVA)) with respect to V. (**c**) Western blot analyses of JAK2 and STAT5 in spleen from *Gata1^{low}* mice treated either with vehicle (V) or Rux (T) (each lane a separate animal). Quantification of results obtained with three to four mice per group is presented on the right. *P*-values were calculated by ANOVA. (**d**) Representative hematoxylin–eosin (top and middle panels on the left) and Gomori silver (bottom panels on the left) stains of bone marrow and spleen sections from *Gata1^{low}* mice treated with either vehicle or Rux, as indicated. Note that the spleen of the Rux-treated mouse presents the typical dark red color of this organ with areas of white pulp (blue circles) appropriately located in germinal centers in the subcapsular area. By contrast, the spleen from vehicle-treated mouse has a disorganized morphology with excessive red pulp areas and paucity of white pulp areas localized mostly in the middle of the parenchyma. Original magnification ×4, ×10 and ×40, as indicated. Representative megakaryocytes are indicated by arrow. (**e**) Computer-assisted quantification of the frequency of megakaryocytes (MK) and of the intensity of Gomori silver staining of bone marrow (BM) and spleen from *Gata1^{low}* mice treated with either vehicle or Rux (three mice per experimental group). *$P < 0.05$ by ANOVA.

Table 2. Treatment of *Gata1^{low}* mice with ruxolitinib decreases splenomegaly but has modest effects on blood values and bone marrow cellularity

Mouse	*Spleen*			*Cells/femur (×10^6)*
	Weight (mg)	*Length (cm)*	*Cells (×10^6)*	
V ($n=6$)	343.3 ± 86.9	2.6 ± 0.2	237.9 ± 79.7	8.6 ± 1.9
T ($n=6$)	231.7 ± 43.1[a]	2.5 ± 0.3	145.7 ± 66.8[a]	11.5 ± 9.4
WT ($n=12$)	100.0 ± 10.0	NA	159.0 ± 22	16.2 ± 1.8
Gata1^{low}($n=12$)	430.0 ± 45.0	3.1	393.0 ± 38.0	9.7 ± 0.7

Abbreviations: NA, not available; T, treatment; V, vehicle; WT, wild type. [a]Value statistically different ($P < 0.05$) from those observed in wild-type mice.

for a duration similar to that investigated here for Rux rescued both their abnormal TGF-β signaling and their myelofibrotic phenotype.[15,16] To gain insights on the mechanism of action of Rux in this animal model, we investigated the levels of TGF-β in the bone marrow and the spleen of *Gata1^{low}* mice treated either with Rux or with vehicle (Figure 4). As expected,[16] by immunohistochemistry both bone marrow and spleen from vehicle-treated *Gata1^{low}* mice expressed great levels of TGF-β, and the

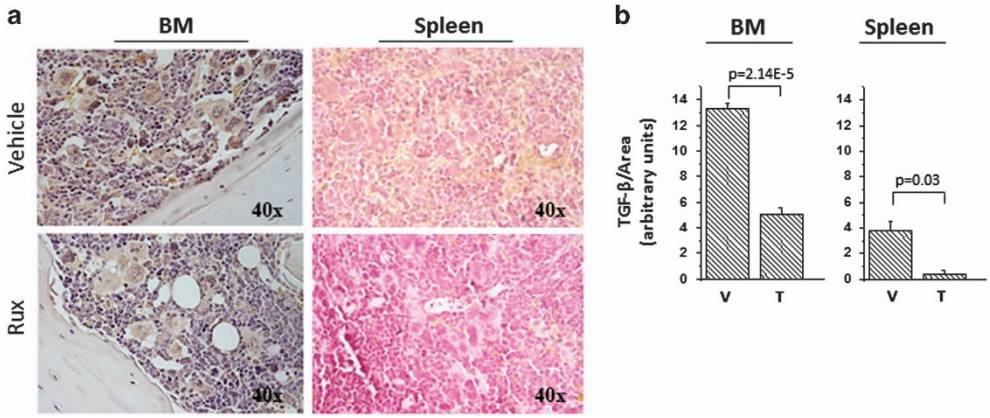

Figure 4. Rux decreases the TGF-β content of the bone marrow and the spleen from *Gata1*^{low} mice. (**a**) Representative immunostaining with TGF-β antibodies of bone marrow (BM) and spleen sections from *Gata1*^{low} mice treated with either vehicle or Rux, as indicated. Magnification ×40. (**b**) Computer-assisted quantification of the intensity of TGF-β immunostaining of bone marrow and spleen sections of the groups presented in **a**. Results are presented as mean (± s.d.) of those obtained by evaluating three to four sections per mouse, three mice per group. *P*-values were calculated by analysis of variance.

staining was mainly localized with the megakaryocytes (Figures 4a and b). Treatment with Rux decreased by threefold the levels of TGF-β detected in the bone marrow and down to barely detectable in the spleen. The greater effects exerted by Rux on the levels of TGF-β present in the spleen than in the bone marrow are consistent with the fact that this treatment significantly reduced the frequency of megakaryocytes only in the spleen.

In conclusion, these results indicate that Rux rescues the myelofibrotic traits, normalizing the TGF-β of the spleen but is only partially effective in rescuing the defective hematopoiesis of the bone marrow from *Gata1*^{low} mice.

Gata1^{low} mice express a ribosomal signature predictive of ribosomal deficiency

We have previously demonstrated that although megakaryocytes from *Gata1*^{low} mice contain levels of *Gata1* mRNA only twofold lower than normal, the GATA1 protein in these cells is barely detectable.[7,9] We had attributes this discrepancy to a predicted low sensitivity of immunohistochemistry. However, the demonstration that activation of TPO/MPL/JAK2 signaling induces a ribosomal deficiency within megakaryocytes derived from MF patient stem cells, which hampers *GATA1* mRNA translation in *ex vivo*-expanded megakaryocytes,[5] and the realization that *Gata1*^{low} mice express an activated TPO pathway (this manuscript) made us question the original hypothesis that reduced content of GATA1 in *Gata1*^{low} megakaryocytes is solely the consequence of deletion of the lineage-specific enhancer. To clarify this point we performed microarray analyses of the bone marrow and the spleen from *Gata1*^{low} and wild-type littermates of comparable age (all 10- to 13-month-old males). This analysis identified differential expression of numerous genes between *Gata1*^{low} and wild-type littermates. The majority of these genes were in pathways related to inflammation/autoimmunity, including the TGF-β pathway (see GSE89630). Among the differentially expressed genes in the bone marrow, there was a strong discordant ribosome signature, which reached statistical significance for two genes of the large subunit (*RLP36AL* and *RPL27A*, both activated in *Gata1*^{low} bone marrow) and four genes (*RSP6KA1* and *RSP9* activated; *RSP24* and *RSP26* repressed) of the small subunit (Figure 5a). In addition, there was a significant decline in the mRNA levels for the ribosome maturation protein SBDS, which has been implicated in the joining of the 40S and 60S subunits during the ribosome biogenesis.[40] Of interest, hypomorphic mutations of RSP24 and RSP26 are observed in a subset of patients with Diamond Blackfan anemia, a disease due to inefficient translation of GATA1 mRNA,[41] and loss-of-function mutation of SBDS are associated with the Shwachman–Diamond syndrome,[42] one of the inherited bone marrow failure syndromes with a disease manifestation predictive of ribosomopathy.

A limitation of these results is that they were obtained on mRNA prepared from the entire tissue and therefore were not selective to megakaryocytes. This caveat was addressed by performing a careful electron microscopy study, which confirmed that the cytoplasm of megakaryocytes from *Gata1*^{low} mice contain a poorly developed endoplasmic reticulum with rare isolated polysomes, a clear indication of reduced ribosome biogenesis (Figure 5c).

Next, we used gene set enrichment analysis[22] to identify pathways that are dysregulated in bone marrow and spleen cells of *Gata1*^{low} mice. As expected, we observed significant enrichment of a gene set derived from a set of known GATA1 erythroid cell target genes in cells from the bone marrow (Figures 6a and c). Among other gene sets (Supplementary Table S1), we also observed enrichment of the *RPS14* gene signature, which was derived from the changes seen upon knockdown of RPS14 in erythroid cells[43] (Figures 6b and d). In contrast, we did not detect significant changes in ribosome gene mRNA levels (Figure 5b) or downregulation of the RPS14 pathway in the spleen of *Gata1*^{low} mice (data not shown). Gene set enrichment analysis further revealed that additional enriched pathways include the cell cycle (including E2F and RB) and transcription, such as GLI1 and HOXA9, the nuclear translocation of which is regulated by TPO[44] (Supplementary Table S1).

Together, these results suggest that as observed in the patients,[5] activation of the TPO/MPL pathway, through mechanism(s) still unclear, induces in *Gata1*^{low} mice a RSP14 deficiency, which contributes to reduce the GATA1 content in the megakaryocytes of these mice. Reduction of GATA1 content then likely contributes to exacerbate the ribosomal gene defect, perhaps by directly regulating expression of a subset of ribosome genes. Indeed, a recent report showed that GATA1 binds to a subset of ribosome genes, including *RPS19* and *RPS26*.[45]

DISCUSSION

In this manuscript, by showing that *Gata1*^{low} mice express a hyperactive TPO/MPL axis, we provide new insights on the mechanism(s) that leads to recovery from chronic anemia, on the differences between regulation of *Gata1* in erythroid cells and

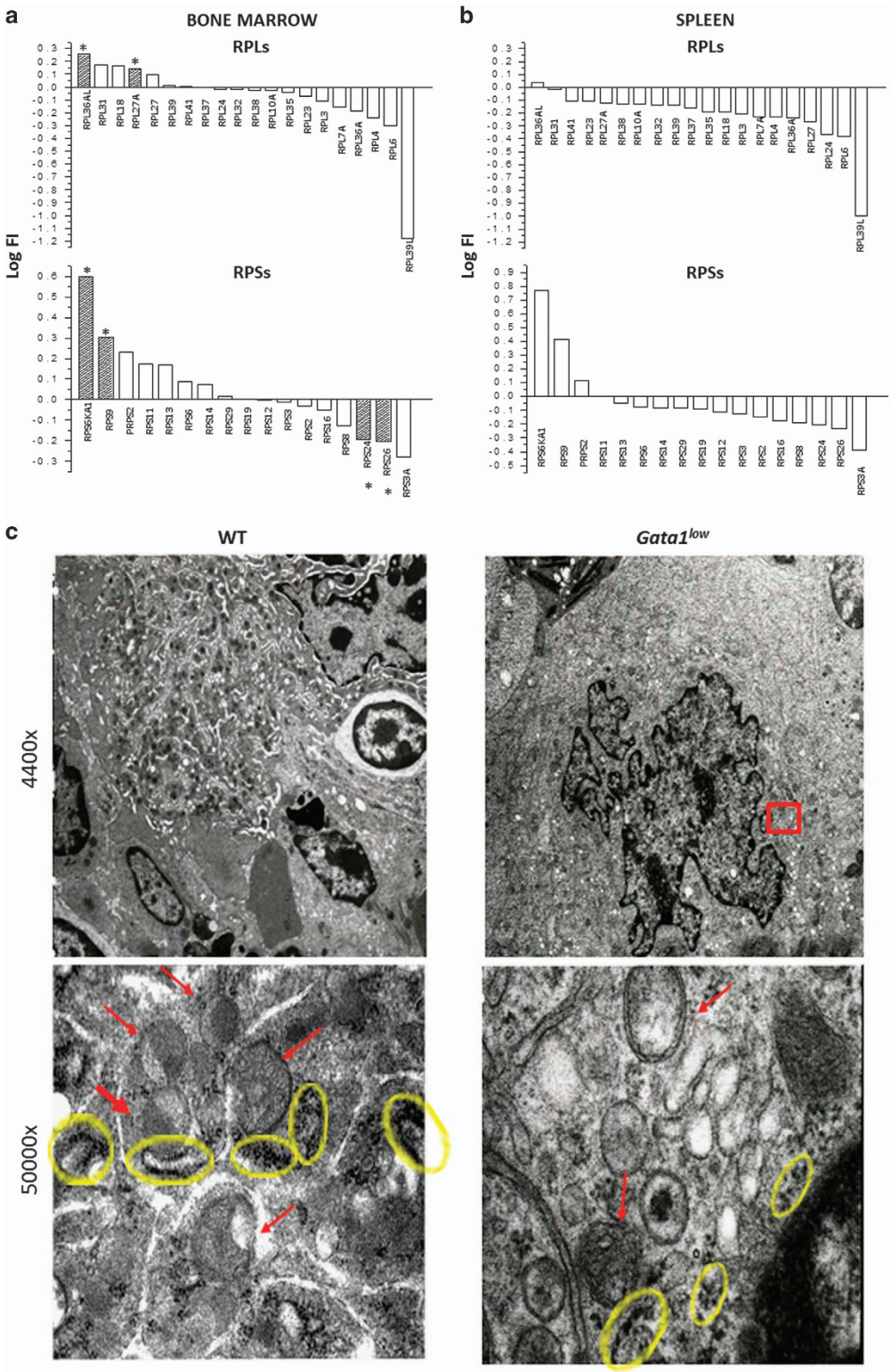

Figure 5. Bone marrow from *Gata1^{low}* mice express a discordant ribosomal signature and contain megakaryocytes with poorly developed endoplasmic reticulum and reduced numbers of polysomes. Summary of the fold-change with respect to wild type in the expression of genes for the large (top) and small (bottom) subunit of the ribosomes in bone marrow (**a**) and spleen (**b**) from *Gata1^{low}* mice. Results are expressed as log fold increase. Value statistically different ($P < 0.05$) from those observed in wild-type mice are indicated by *. (**c**) Transmission electron microscopy of representative megakaryocytes from wild-type (WT) and *Gata1^{low}* littermates. Megakaryocytes were recognized by their distinctive morphology shown in the low magnification presented in the top panels. Details of the perinuclear area of the cells (indicated by the red square) showing the poorly developed rough endoplasmic reticulum with reduced numbers of polysomes (indicated by the yellow circles) are shown in the photographs obtained at greater magnification in the bottom panels. To be noted that the *Gata1^{low}* megakaryocyte is smaller and less mature than the wild-type one. Similar results were obtained by analyzing at least five separate megakaryocytes from three mice per group.

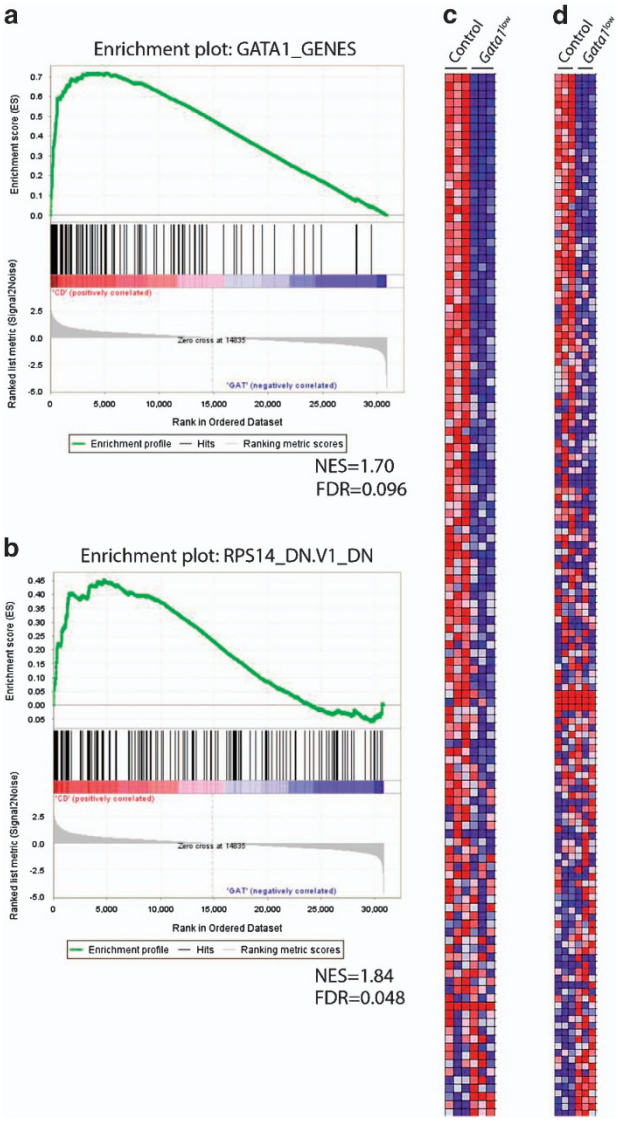

Figure 6. The GATA1 and RPS14 gene signatures are enriched in *Gata1*^{low} bone marrow. Gene set enrichment analysis (GSEA) revealed that the GATA1 and RPS14 gene signatures are enriched in *Gata1*^{low} mice. (**a**, **b**) GSEA plots for GATA1 (**a**) and RPS14 (**b**) signatures. (**c**, **d**) Heat maps of differentially expressed genes in the GATA1 (**c**) and the RPS14 (**d**) signatures.

megakaryocytes, and on our understanding on how to ameliorate therapies for MF.

Seminal work by Dr Paulson has clarified how the combination of BMP4, soluble stem cell factor and glucocorticoid receptor signaling activates microenvironmental cues in the spleen, which allows recovering from acute stress.[10] By contrast, the mechanisms that lead to recovery from chronic stress, such as those that mediates the expansion of the erythroid compartments in congenic hemoglobinopathies, or during chronic inflammation, are still poorly understood. Studies from the Rivella laboratory had indicated that to recover from chronic anemia, mice, and possibly humans, activate a pathological interaction between erythroblasts and their macrophage niches, which leads to ineffective erythropoiesis.[46] This interaction is restricted by treatment with Rux, indicating that is sustained by JAK signaling activated by unknown cytokines. Also *Gata1*^{low} mice suffer from chronic anemia, which is compensated by extramedullary hematopoiesis in the spleen. The data presented in this manuscript suggest that the chronic stress pathway in the spleen is activated by TPO and its downstream JAK-dependent signaling.

The regulatory regions of the *Gata1* gene include three hypersensitive sites (HSs).[47] The hypomorphic *Gata1*^{low} mutation deletes the distal HS1 sites[12] and reduces by two- to threefold the levels of *Gata1* mRNA in the bipotential megakaryocytic/erythroid progenitor cells, in erythroid cells, megakaryocytes and dendritic cells.[20] The mice are born anemic but those that may activate efficiently extramedullary hematopoiesis in the spleen remain thrombocytopenic, recover from anemia soon after birth and have a normal lifespan.[7] As GATA1 is indispensable for erythroid maturation, the question is raised on the mechanisms that rescue erythropoiesis in the spleen of these animals. In addition to HS1, the *Gata1* gene contains an additional enhancer HS2. By using a reporter gene driven by HS2, we demonstrated that HS2 is active in erythroid and megakaryocytes from the spleen, but not in those from the bone marrow indicating that activation of mRNA translation from this alternative site may rescue Gata1 deficiency in the spleen.[48] However, although HS2 is active both in erythroid cells and megakaryocytes, erythroid cells from the spleen contain normal levels of GATA1 protein while the levels of GATA1 protein detectable by immunohistochemistry in megakaryocytes remain low.[7,9] This observation raises the question on the mechanism that reduces the GATA1 protein in the megakaryocytes from the spleen in this mouse model. The microarray analyses described in this paper indicate that the bone marrow, which contains mainly megakaryocytes, express a ribosomal deficiency while the spleen, which contain mainly erythroblasts, does not. In addition, electron microscopy observation indicated that megakaryocytes from both bone marrow and spleen have a poorly developed rough endoplasmic reticulum and contain few ribosomes. These observations suggest that as in myelofibrotic patients, in *Gata1*^{low} mice an activated TPO/MPL axis induces a ribosomal deficiency in the megakaryocytes, but not in the erythroid cells, which results in thrombocytopenia due to reduced *Gata1* mRNA translation.

MF is the most severe of the Philadelphia chromosome-negative myeloproliferative neoplasms and is characterized by a wide range of constitutional symptoms and short survival.[49] Although a large European study found that the median survival of patients with MF has improved from 4.6 years in 1980–1995 to 6.5 years in 1996–2007, long-term survival of these patients remains low.[50] In 2005, the discovery of the activating *JAK2*V617F mutation in ~50–60% of the patients with MF[51–54] led to the development of a number of pharmacological inhibitors of Janus Kinases for the treatment of this disease. However, despite the large numbers of JAK inhibitors that were developed and tested for the treatment of MF, only one, Rux, was demonstrated by the large COMFORT clinical trial to markedly improve splenomegaly and MF-associated symptoms over placebo or best available therapy[55,56], and has been approved by the Food and Drug Administration for clinical use in this disease.[57] Many other JAK inhibitors have been discontinued or are under consideration for other indications related to chronic inflammation, such as rheumatoid arthritis.[58] However, even Rux has modest effects on bone marrow fibrosis and does not decrease the mutant JAK2 allele burden,[57] leading to questions whether this agent is a truly modifying agent in MF. Although multiple analyses of the Rux trials have shown a survival advantage for Rux -treated patients,[55,56] it has been argued that the drug may improve survival by improving appetite, weight and correcting cachexia as a result of a robust suppression on inflammatory cytokines some of which have been shown as independent predictors of poor survival in MF.[59] It is currently debated whether Rux may exert some of its functions indirectly, by inhibiting JAK signaling mediated by the pro-inflammatory milieu of the microenvironment.

Although Rux does not affect ALK5 (IC60 = 6907 nM),[60] the TGF-β receptor 1 kinase whose inhibition rescued MF in *Gata1*^{low} mice,

treatment with Rux exerted on the phenotype of *Gata1^{low}* mice results very similar to those observed in the patients: it reduced spleen size and normalized the cellular architecture of this organ but did not significantly reduced bone marrow fibrosis. Of interest however, it decreased the megakaryocytes and TGF-β content of the spleen, suggesting that it mediates its effects indirectly by normalizing the cellular populations responsible for abnormal TGF-β production in this organ. These results suggest that combination therapy with inhibitors of JAK and TGF-β may be beneficial in the treatment of MF.

In conclusion, these results validate the *Gata1^{low}* model as a bona fide model of MF by indicating that these mice express an activated TPO/MPL axis and an abnormal ribosomal signature, which may contribute to reduced expression of GATA1 in megakaryocytes by reducing the efficiency of its mRNA translation.

CONFLICT OF INTEREST

The authors declare no conflict of interest.

ACKNOWLEDGEMENTS

This study was supported by grants from the National Cancer Institute (P01-CA108671) and Associazione Italiana Ricerca sul Cancro (AIRC 17608). We acknowledge Dr Ilaria Ceglia for performing the functional annotation clustering of the microarray data, Dr Janis Abkowitz and Raymond Doty for providing the GATA1 gene set, and Kirin Pharmaceuticals for providing the Mpl antibody AMM2.

AUTHOR CONTRIBUTIONS

MZ, LC, FM, FC, MM and LV performed experiments and analyzed data; CZ performed the gene set enrichment analyses; RAR, JDC and ARM designed research, analyzed the data and wrote the manuscript. All the authors have read the manuscript, concur with its content and state that its content has not been submitted elsewhere.

REFERENCES

1 Grinfeld J, Nangalia J, Green AR. Molecular determinants of pathogenesis and clinical phenotype in myeloproliferative neoplasms. *Haematologica* 2017; **102**: 7–17.
2 Cerutti A, Custodi P, Duranti M, Noris P, Balduini CL. Thrombopoietin levels in patients with primary and reactive thrombocytosis. *Br J Haematol* 1997; **99**: 281–284.
3 Vannucchi AM, Pancrazzi A, Guglielmelli P, Di Lollo S, Bogani C, Baroni G *et al.* Abnormalities of GATA-1 in megakaryocytes from patients with idiopathic myelofibrosis. *Am J Pathol* 2005; **167**: 849–858.
4 Gilles L, Arslan AD, Konstantinoff K, McNulty M, Terra L, Pardanani A *et al.* Defect in ribosome biogenesis contributes to impaired megakaryopoiesis in primary myelofibrosis. *Blood* 2014; **124**: (abstract 4584).
5 Gilles L, Arslan AD, Marinaccio C, Wen QJ, Arya P, McNulty M *et al.* Downregulation of GATA1 drives impaired hematopoiesis in primary myelofibrosis. *J Clin Invest* 2017; **127**: 1316–1320.
6 Vyas P, Ault K, Jackson CW, Orkin SH, Shivdasani RA. Consequences of GATA-1 deficiency in megakaryocytes and platelets. *Blood* 1999; **93**: 2867–2875.
7 Vannucchi AM, Bianchi L, Cellai C, Paoletti F, Rana RA, Lorenzini R *et al.* Development of myelofibrosis in mice genetically impaired for GATA-1 expression (GATA-1(low) mice). *Blood* 2002; **100**: 1123–1132.
8 Vannucchi AM, Paoletti F, Linari S, Cellai C, Caporale R, Ferrini PR *et al.* Identification and characterization of a bipotent (erythroid and megakaryocytic) cell precursor from the spleen of phenylhydrazine-treated mice. *Blood* 2000; **95**: 2559–2568.
9 Sanchez M, Weissman IL, Pallavicini M, Valeri M, Guglielmelli P, Vannucchi AM *et al.* Differential amplification of murine bipotent megakaryocytic/erythroid progenitor and precursor cells during recovery from acute and chronic erythroid stress. *Stem Cells* 2006; **24**: 337–348.
10 Paulson RF, Shi L, Wu DC. Stress erythropoiesis: new signals and new stress progenitor cells. *Curr Opin Hematol* 2011; **18**: 139–145.
11 Belay E, Miller CP, Kortum AN, Torok-Storb B, Blau CA, Emery DW. A hyperactive Mpl-based cell growth switch drives macrophage-associated erythropoiesis through an erythroid-megakaryocytic precursor. *Blood* 2015; **125**: 1025–1033.
12 McDevitt MA, Shivdasani RA, Fujiwara Y, Yang H, Orkin SH. A 'knockdown' mutation created by cis-element gene targeting reveals the dependence of erythroid cell maturation on the level of transcription factor GATA-1. *Proc Natl Acad Sci USA* 1997; **94**: 6781–6785.
13 Martelli F, Ghinassi B, Panetta B, Alfani E, Gatta V, Pancrazzi A *et al.* Variegation of the phenotype induced by the Gata1low mutation in mice of different genetic backgrounds. *Blood* 2005; **106**: 4102–4113.
14 Alexander WS, Roberts AW, Nicola NA, Li R, Metcalf D. Deficiencies in progenitor cells of multiple hematopoietic lineages and defective megakaryocytopoiesis in mice lacking the thrombopoietic receptor c-Mpl. *Blood* 1996; **87**: 2162–2170.
15 Quintas-Cardama A, Vaddi K, Liu P, Manshouri T, Li J, Scherle PA *et al.* Preclinical characterization of the selective JAK1/2 inhibitor INCB018424: therapeutic implications for the treatment of myeloproliferative neoplasms. *Blood* 2010; **115**: 3109–3117.
16 Zingariello M, Martelli F, Ciaffoni F, Masiello F, Ghinassi B, D'Amore E *et al.* Characterization of the TGF-beta1 signaling abnormalities in the Gata1low mouse model of myelofibrosis. *Blood* 2013; **121**: 3345–3363.
17 Spangrude GJ, Lewandowski D, Martelli F, Marra M, Zingariello M, Sancillo L *et al.* P-selectin sustains extramedullary hematopoiesis in the Gata1 low model of myelofibrosis. *Stem Cells* 2016; **34**: 67–82.
18 Kai M, Hagiwara T, Emuta C, Chisaka Y, Tsuruhata K, Endo C *et al.* In vivo efficacy of anti-MPL agonist antibody in promoting primary human hematopoietic cells. *Blood* 2009; **113**: 2213–2216.
19 Yoshihara H, Arai F, Hosokawa K, Hagiwara T, Takubo K, Nakamura Y *et al.* Thrombopoietin/MPL signaling regulates hematopoietic stem cell quiescence and interaction with the osteoblastic niche. *Cell Stem Cell* 2007; **1**: 685–697.
20 Ghinassi B, Sanchez M, Martelli F, Amabile G, Vannucchi AM, Migliaccio G *et al.* The hypomorphic Gata1low mutation alters the proliferation/differentiation potential of the common megakaryocytic-erythroid progenitor. *Blood* 2007; **109**: 1460–1471.
21 Migliaccio AR, Martelli F, Verrucci M, Migliaccio G, Vannucchi AM, Ni H *et al.* Altered SDF-1/CXCR4 axis in patients with primary myelofibrosis and in the Gata1 low mouse model of the disease. *Exp Hematol* 2008; **36**: 158–171.
22 Subramanian A, Tamayo P, Mootha VK, Mukherjee S, Ebert BL, Gillette MA *et al.* Gene set enrichment analysis: a knowledge-based approach for interpreting genome-wide expression profiles. *Proc Natl Acad Sci USA* 2005; **102**: 15545–15550.
23 de Sauvage FJ, Hass PE, Spencer SD, Malloy BE, Gurney AL, Spencer SA *et al.* Stimulation of megakaryocytopoiesis and thrombopoiesis by the c-Mpl ligand. *Nature* 1994; **369**: 533–538.
24 Ghinassi B, Zingariello M, Martelli F, Lorenzini R, Vannucchi AM, Rana RA *et al.* Increased differentiation of dermal mast cells in mice lacking the Mpl gene. *Stem Cells Dev* 2009; **18**: 1081–1092.
25 Martelli F, Ghinassi B, Lorenzini R, Vannucchi AM, Rana RA, Nishikawa M *et al.* Thrombopoietin inhibits murine mast cell differentiation. *Stem Cells* 2008; **26**: 912–919.
26 Kaser A, Brandacher G, Steurer W, Kaser S, Offner FA, Zoller H *et al.* Interleukin-6 stimulates thrombopoiesis through thrombopoietin: role in inflammatory thrombocytosis. *Blood* 2001; **98**: 2720–2725.
27 Wendling F. Thrombopoietin: its role from early hematopoiesis to platelet production. *Haematologica* 1999; **84**: 158–166.
28 Kaushansky K. Historical review: megakaryopoiesis and thrombopoiesis. *Blood* 2008; **111**: 981–986.
29 Gurney AL, Carver-Moore K, de Sauvage FJ, Moore MW. Thrombocytopenia in c-mpl-deficient mice. *Science* 1994; **265**: 1445–1447.
30 Shivdasani RA, Fielder P, Keller GA, Orkin SH, de Sauvage FJ. Regulation of the serum concentration of thrombopoietin in thrombocytopenic NF-E2 knockout mice. *Blood* 1997; **90**: 1821–1827.
31 Fielder PJ, Gurney AL, Stefanich E, Marian M, Moore MW, Carver-Moore K *et al.* Regulation of thrombopoietin levels by c-mpl-mediated binding to platelets. *Blood* 1996; **87**: 2154–2161.
32 Villeval JL, Cohen-Solal K, Tulliez M, Giraudier S, Guichard J, Burstein SA *et al.* High thrombopoietin production by hematopoietic cells induces a fatal myeloproliferative syndrome in mice. *Blood* 1997; **90**: 4369–4383.
33 Kaushansky K. The molecular mechanisms that control thrombopoiesis. *J Clin Invest* 2005; **115**: 3339–3347.
34 Moliterno AR, Hankins WD, Spivak JL. Impaired expression of the thrombopoietin receptor by platelets from patients with polycythemia vera. *N Engl J Med* 1998; **338**: 572–580.
35 Yoon SY, Li CY, Tefferi A. Megakaryocyte c-Mpl expression in chronic myeloproliferative disorders and the myelodysplastic syndrome: immunoperoxidase staining patterns and clinical correlates. *Eur J Haematol* 2000; **65**: 170–174.

36 Koppikar P, Levine RL. JAK2 and MPL mutations in myeloproliferative neoplasms. *Acta Haematol* 2008; **119**: 218–225.
37 Zingariello M, Ruggeri A, Martelli F, Marra M, Sancillo L, Ceglia I *et al.* A novel interaction between megakaryocytes and activated fibrocytes increases TGF-beta bioavailability in the Gata1(low) mouse model of myelofibrosis. *Am J Blood Res* 2015; **5**: 34–61.
38 Ciaffoni F, Cassella E, Varricchio L, Massa M, Barosi G, Migliaccio AR. Activation of non-canonical TGF-beta1 signaling indicates an autoimmune mechanism for bone marrow fibrosis in primary myelofibrosis. *Blood Cells Mol Dis* 2015; **54**: 234–241.
39 Korus M, Mahon GM, Cheng L, Whitehead IP. p38 MAPK-mediated activation of NF-kappaB by the RhoGEF domain of Bcr. *Oncogene* 2002; **21**: 4601–4612.
40 Burwick N, Shimamura A, Liu JM. Non-Diamond Blackfan anemia disorders of ribosome function: Shwachman Diamond syndrome and 5q- syndrome. *Semin Hematol* 2011; **48**: 136–143.
41 Danilova N, Gazda HT. Ribosomopathies: how a common root can cause a tree of pathologies. *Dis Model Mech* 2015; **8**: 1013–1026.
42 Zambetti NA, Bindels EM, Van Strien PM, Valkhof MG, Adisty MN, Hoogenboezem RM *et al.* Deficiency of the ribosome biogenesis gene Sbds in hematopoietic stem and progenitor cells causes neutropenia in mice by attenuating lineage progression in myelocytes. *Haematologica* 2015; **100**: 1285–1293.
43 Ebert BL, Pretz J, Bosco J, Chang CY, Tamayo P, Galili N *et al.* Identification of RPS14 as a 5q- syndrome gene by RNA interference screen. *Nature* 2008; **451**: 335–339.
44 Kirito K, Fox N, Kaushansky K. Thrombopoietin induces HOXA9 nuclear transport in immature hematopoietic cells: potential mechanism by which the hormone favorably affects hematopoietic stem cells. *Mol Cell Biol* 2004; **24**: 6751–6762.
45 Amanatiadou EP, Papadopoulos GL, Strouboulis J, Vizirianakis IS. GATA1 and PU.1 bind to ribosomal protein genes in erythroid cells: implications for ribosomopathies. *PLoS One* 2015; **10**: e0140077.
46 Ramos P, Casu C, Gardenghi S, Breda L, Crielaard BJ, Guy E *et al.* Macrophages support pathological erythropoiesis in polycythemia vera and beta-thalassemia. *Nat Med* 2013; **19**: 437–445.
47 Vyas P, McDevitt MA, Cantor AB, Katz SG, Fujiwara Y, Orkin SH. Different sequence requirements for expression in erythroid and megakaryocytic cells within a regulatory element upstream of the GATA-1 gene. *Development* 1999; **126**: 2799–2811.
48 Migliaccio AR, Martelli F, Verrucci M, Sanchez M, Valeri M, Migliaccio G *et al.* Gata1 expression driven by the alternative HS2 enhancer in the spleen rescues the hematopoietic failure induced by the hypomorphic Gata1low mutation. *Blood* 2009; **114**: 2107–2120.
49 Tefferi A, Skoda R, Vardiman JW. Myeloproliferative neoplasms: contemporary diagnosis using histology and genetics. *Nat Rev Clin Oncol* 2009; **6**: 627–637.
50 Cervantes F, Dupriez B, Passamonti F, Vannucchi AM, Morra E, Reilly JT *et al.* Improving survival trends in primary myelofibrosis: an international study. *J Clin Oncol* 2012; **30**: 2981–2987.
51 Baxter EJ, Scott LM, Campbell PJ, East C, Fourouclas N, Swanton S *et al.* Acquired mutation of the tyrosine kinase JAK2 in human myeloproliferative disorders. *Lancet* 2005; **365**: 1054–1061.
52 James C, Ugo V, Le Couedic JP, Staerk J, Delhommeau F, Lacout C *et al.* A unique clonal JAK2 mutation leading to constitutive signalling causes polycythaemia vera. *Nature* 2005; **434**: 1144–1148.
53 Levine RL, Wadleigh M, Cools J, Ebert BL, Wernig G, Huntly BJ *et al.* Activating mutation in the tyrosine kinase JAK2 in polycythemia vera, essential thrombocythemia, and myeloid metaplasia with myelofibrosis. *Cancer Cell* 2005; **7**: 387–397.
54 Kralovics R, Passamonti F, Buser AS, Teo SS, Tiedt R, Passweg JR *et al.* A gain-of-function mutation of JAK2 in myeloproliferative disorders. *N Engl J Med* 2005; **352**: 1779–1790.
55 Cervantes F, Vannucchi AM, Kiladjian JJ, Al-Ali HK, Sirulnik A, Stalbovskaya V *et al.* Three-year efficacy, safety, and survival findings from COMFORT-II, a phase 3 study comparing ruxolitinib with best available therapy for myelofibrosis. *Blood* 2013; **122**: 4047–4053.
56 Vannucchi AM, Kantarjian HM, Kiladjian JJ, Gotlib J, Cervantes F, Mesa RA *et al.* A pooled analysis of overall survival in COMFORT-I and COMFORT-II, 2 randomized phase III trials of ruxolitinib for the treatment of myelofibrosis. *Haematologica* 2015; **100**: 1139–1145.
57 Mascarenhas J, Hoffman R. A comprehensive review and analysis of the effect of ruxolitinib therapy on the survival of patients with myelofibrosis. *Blood* 2013; **121**: 4832–4837.
58 van Vollenhoven RF, Fleischmann R, Cohen S, Lee EB, Garcia Meijide JA, Wagner S *et al.* Tofacitinib or adalimumab versus placebo in rheumatoid arthritis. *N Engl J Med* 2012; **367**: 508–519.
59 Tefferi A, Vaidya R, Caramazza D, Finke C, Lasho T, Pardanani A. Circulating interleukin (IL)-8, IL-2R, IL-12, and IL-15 levels are independently prognostic in primary myelofibrosis: a comprehensive cytokine profiling study. *J Clin Oncol* 2011; **29**: 1356–1363.
60 Asshoff M, Petzer V, Warr MR, Haschka D, Tymoszuk P, Demetz E *et al.* Momelotinib inhibits ACVR1/ALK2, decreases hepcidin production and ameliorates anemia of chronic disease in rodents. *Blood* 2017; **129**: 1823–1830.

Supplementary Information accompanies this paper on Blood Cancer Journal website (http://www.nature.com/bcj)